

Supplementary Information

To generate the following plots we used the complete data cohort (September 2016 - February 2021), and their respective events and information reported by the time of the submission (March 2021).

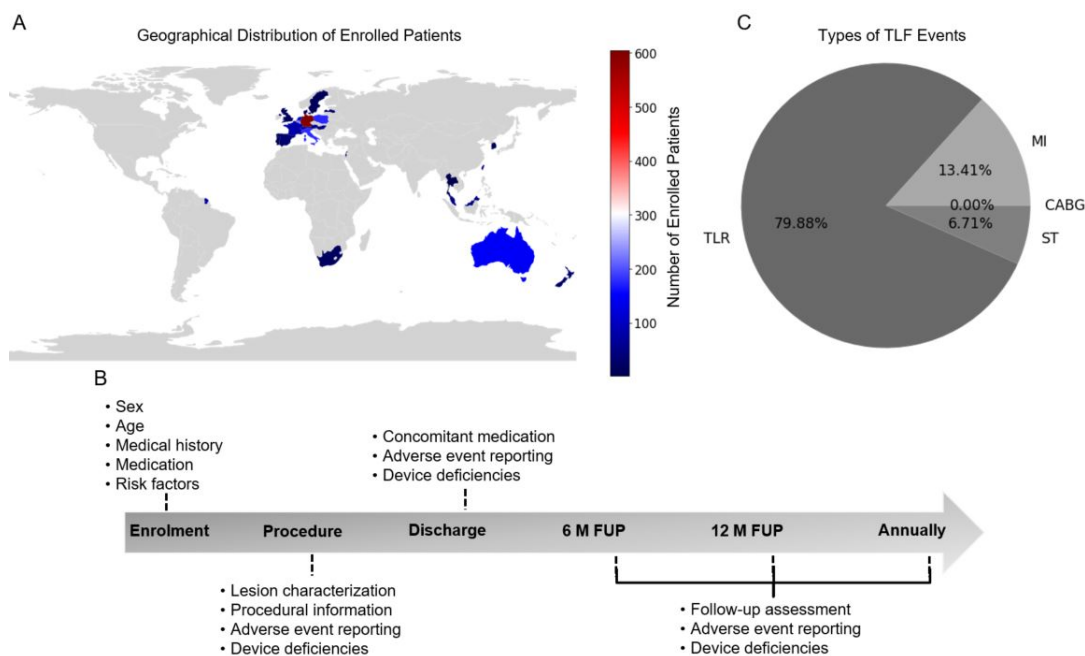


Figure S1. Overview of BIOSOLVE-IV post-market study. (A) Number of enrolled patient per country. (B) Study timeline and collected information. (C) Distribution of all occurred TLF-causing events. MI = myocardial infarction, ST = stent thrombosis, TLR = target lesion revascularization.

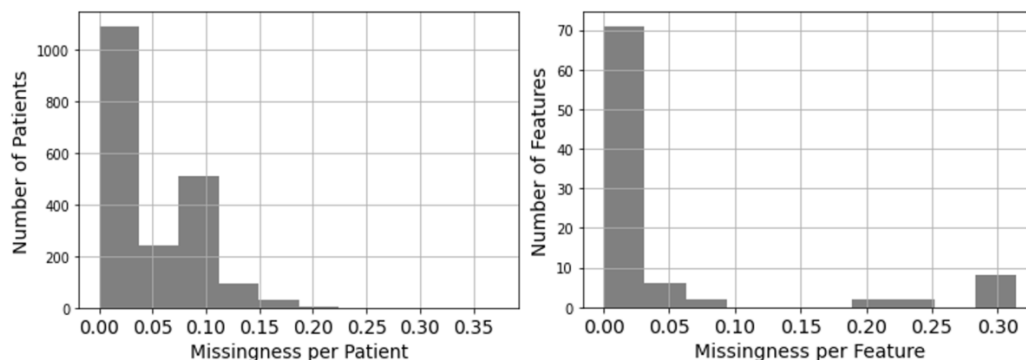


Figure S2. The missingness in the BIOSOLVE-IV study is low with a missingness rate < 0.2 for 75.0% of the patients and < 0.1 for 85.0% of the features. (A) The figure shows the missingness rate per patient. Most of the patients (approx. 1,400) had a missingness rate between 0.0-20.0%. The few patients with a missingness rate $\geq 50.0\%$ were excluded. (B) Most of the features were available for all patients. There are only 7 features missing for about 25.0-30.0% of all patients.

Paper	Outcome	Predictors	Paper	Outcome	Predictors
		Predictor p-value			Predictor p-value
Alaa, 2019 [16]	CAD	Age (m/w)	Stolker, 2010 [EVENT] [21]	TLR	Age <60 y
		Smoking (m/w)			Prior PCI(s)
		Unusual walking pace (m/w)			Left main PCI
		SBP (m/w)			SVG location
		Ankle spacing width (w)			Min. stent diameter ≤ 2.5 mm
		Microalbumin in urine (m)			Total stent length ≥ 40 mm
		BMI (m)			Diabetes mellitus (30d-1y)
D'Agostino Sr, 2008 [Framingham Risk Score] [12]	CVD	Age	Konigstein, 2019 [15]	TLF	hypertension (30d-1y)
		Total cholesterol			Moderate/severe calcification (30d-1y)
		Smoking			RVD ((30d-1y)/[1y-5y])
		Diabetes mellitus			DS (postprocedure) (per %) (30d-1y)
Sampedo-Gómez, 2020 [17]	SR	Lower post-PCI MLD, mm	Anadol, 2020 [14]	TLF	Total stent length [mm] ([0-30d]/[30d-1y])
		Post-PCI stenosis, %			Prior CABG (1-5y)
		Diabetes mellitus			Prior PCI (1-5y)
		≥ 2 vessel CVD			Scaffold footprint (<1y)
		Abnormal total cholesterol			Optimal implementation (<1y)
		# Implanted stents			RVD <2.5mm ([<1y]/[2-3y])
		Post-PCI thrombus			Diabetes mellitus (4y-5y)
Singh, 2004 [PRESTO-1, PRESTO-2] [11, 20]	SR	Post-PCI TIMI flow			eGFR (4y-5y)
		Current smoker *, ^			RVD ≥ 3.5 mm
		Hypertension			
		Prior CABG			
		Prior PCI(s) *, ^			
		Diabetes mellitus ^			
		Current unstable angina*			
Cassese, 2004 [22]	SR	Lesion length >20mm *, ^			
		ACC/AHA type C lesion *, ^			
		Female gender *			
		Diabetes mellitus			
		Prior CABG			
		NSTEMI			
		STEMI			
		≥ 2 vessel CVD			
		Left main target vessel			
		Left circumflex coronary artery			
		Complex (type B2/C) lesion			
		Chronic occlusion			
		Lesion length			
		Vessel size			
		Initial diameter stenosis			
		Maximal balloon diameter			
		Maximal balloon pressure			
		Balloon-to-vessel ratio			

Table S1. Overview of significant predictors of cardio vascular disease in literature. Other studies used univariate or multivariate analysis. TLR = target lesion revascularization, SR = stent restenosis, SBP = systolic blood pressure, MLD = minimal lumen diameter, SVG = saphenous vein graft, RVD = reference vessel diameter, DS = diameter stenosis, Scaffold footprint = expresses the maximum percentage of the circumference of the vessel occupied by struts, optimal implantation technique includes pre-dilatation, proper sizing and post-dilatation. Bold **features** are used by Framingham score. * = used by PRESTO-1, ^ = used by PRESTO-2

Feature		TLF (n=163)	No TLF (n=1811)	Total (n=1975)	p-value	Missingness [%]
Age (years)		60.15±10.94	61.97±10.48	61.82±10.51	0.03	0.00
Male		137 (83.54%)	1326 (73.10%)	1463 (73.96%)	<0.01	0.00
EQ5D questionnaire*	Mobility*	1	1	1	0.76	31.50
	Self-care*	1	1	1	0.77	31.50
	Usual activities*	1	1	1	0.97	31.50
	Pain/discomfort*	1	1	1	0.88	31.50
	Anxiety/depression*	1	1	1	0.60	31.50
Prior MI		31 (18.90%)	386 (21.31%)	418 (21.11%)	0.46	0.10
Type of most recent MI	STEMI	14 (8.54%)	188 (10.38%)	202 (10.23%)	0.72	0.10
	NSTEMI	13 (7.92%)	168 (9.28%)	181 (9.16%)		
Prior stroke/TIA		9 (4.88%)	61 (3.36%)	70 (3.54%)	0.94	0.10
Smoking (current & ex)		95 (57.93%)	1070 (58.99%)	1165 (58.9%)	0.55	0.46
Renal disease		10 (6.1%)	115 (6.34%)	125 (6.32%)	0.90	0.10
Dialysis		0 (0.00%)	0 (0.00%)	0 (0.00%)	1.00	0.10
Hepatic disease		3 (1.83%)	39 (2.15%)	42 (2.12%)	0.78	0.10
Respiratory disease		15 (9.15%)	150 (8.27%)	165 (8.34%)	0.70	0.10
Hypertension		111 (67.68%)	1204 (66.37%)	1315 (66.48%)	0.92	0.00
Hypercholesteremia		113 (68.90%)	1181 (65.10%)	1294 (65.42%)	0.34	0.10
Diabetes melitus		40 (24.39%)	388 (21.39%)	428 (21.64%)	0.66	0.10
Congestive heart failure		17 (10.37%)	140 (7.72%)	157 (7.94%)	0.63	0.10
Number of prior PCI		0.51±1.23	0.48±1.04	0.48±1.306	0.79	0.10
History of cancer		10 (6.1%)	125 (6.89%)	135 (6.83%)	0.95	0.10
Ischemic status	STEMI	0 (0.00%)	7 (0.37%)	7 (0.35%)	0.47	0.15
	NSTEMI	35 (21.34%)	332 (18.33%)	367 (18.58%)		
	CCS Class of stable angina (n=952)*	2	2	2	0.04	0.10
	Unstable angina	34 (20.73%)	315 (17.36%)	349 (17.64%)	0.28	0.10
	Silent ischemia	14 (8.54%)	252 (13.89%)	266 (13.45%)	0.04	0.10
	LVEF class*	1	1	1	0.98	2.98

Table S2. Cohort features (part 1): patient characteristics. * = ordinal data presented as mode, other features represented as mean±SD or absolute number (%), presented p-values are the result of univariate analysis using X^2 test for ordinal and categorical features and point-biserial correlation for continuous features, bold **features** have significant p-value ≤ 0.05 . LVEF = left ventricular ejection fraction

Feature	TLF (n=123)	No TLF (n=1761)	Total (n=1884)	p-value	Missingness [%]
<i>Procedure details</i>					
Duration of procedure [min]	47.87±23.76	47.26±24.10	47.31±24.07	0.76	0.71
Residual stenosis before implantation [%]	12.79±7.59	11.14±8.31	11.26±8.27	0.04	23.76
<i>Device details</i>					
Number of implanted Magmaris scaffolds	1.05±0.24	1.03±0.18	1.03±0.19	0.14	0.25
Maximum pressure applied [atm]	14.2±2.57	14.40±2.73	14.38±2.71	0.38	2.17
Inflation time [sec]	21.46±11.24	23.59±11.23	23.41±11.25	0.02	3.34
Total Magmaris scaffold length [mm]	21.23±6.60	19.98±4.88	20.08±5.05	<0.01	1.57
Magmaris scaffold diameter [mm]	3.23±0.25	3.25±0.25	3.25±0.25	0.29	1.47
Residual stenosis after implantation [%]	1.09±3.59	1.43±4.47	1.40±4.40	0.35	1.77
Device deficiency prior/during procedure	2 (1.22%)	12 (0.66%)	14 (0.71%)	0.41	0.15
<i>Pre-dilatation balloon details</i>					
Number of pre-dilatation balloons	1.45±0.62	1.34±0.60	1.35±0.60	0.03	0.25
Balloon diameter [mm]	3.05±0.31	3.07±0.32	3.07±0.32	0.62	0.46
Balloon length [mm]	14.59±2.91	14.22±2.78	14.25±2.80	0.1	0.51
Number of inflation	1.54±0.64	1.59±1.00	1.58±0.97	0.54	0.66
Maximum pressure [atm]	14.52±3.00	14.64±3.22	14.63±3.20	0.63	0.66
<i>Post-dilatation balloon details</i>					
Number of post-dilatation balloons	1.10±0.55	1.07±0.41	1.07±0.42	0.43	0.30
Balloon diameter [mm]	3.45±0.32	3.45±0.34	3.45±0.34	0.75	4.85
Balloon length [mm]	14.58±3.56	14.19±3.37	14.22±3.37	0.16	4.90
Number of inflations	1.74±1.00	1.88±1.41	1.87±1.39	0.20	5.60
Maximum pressure applied [atm]	16.77±3.08	17.01±3.06	17.00±3.06	0.35	5.11

Table S3. Cohort features (part 2): Procedural information. Features represented as mean±SD or absolute number (%), presented p-values are the result of univariate analysis using point-biserial correlation, bold **features** have significant p-value ≤ 0.05

Feature		TLF (n=163)	No TLF (n=1811)	Total (n=1975)	p-value	Missingness [%]
Lesion location	LAD	107 (65.24%)	887 (48.98%)	994 (50.33%)	< 0.01	0.15
	RCA	43 (26.22%)	525 (28.99%)	568 (28.76%)		
	LCX/LM/RI	14 (8.54%)	399 (21.03%)	413 (20.91%)		
Vessel location	LAD	107 (65.24%)	886 (48.84%)	993 (50.20%)	< 0.01	0.15
	RCA	43 (26.22%)	525 (28.99%)	568 (28.76%)		
	LCX/LM/RI	14 (8.54%)	400 (22.09%)	414 (20.96%)		
Pre-procedure TIMI flow [grade]*		3	3	3	0.07	0.20
ACC / AHA lesion characterization*		2	1	2	0.30	0.20
Moderate/severe lesion calcification		11 (6.71%)	132 (7.28%)	143 (7.23%)	0.90	0.15
Moderate/severe vessel angulation		18 (10.98%)	260 (14.33%)	278 (14.05%)	0.43	0.20
Moderate/excessive vessel tortuosity		10 (6.1%)	224 (12.35%)	234 (11.83%)	0.05	0.25
Bifurcation		4 (2.44%)	85 (4.69%)	89 (4.50%)	0.18	0.20
Eccentric lesions		55 (33.54%)	607 (33.46%)	662 (33.47%)	0.99	0.20
Thrombus		0 (0.00%)	3 (0.17%)	3 (0.15%)	0.60	0.20
Lesion length [mm]		15.43±4.87	14.76±3.86	14.82±3.96	0.04	0.1
Reference vessel diameter [mm]		3.21±0.29	3.24±0.28	3.24±0.28	0.31	0.35
Stenosis pre-procedure in %		82.48±10.43	82.11±10.80	82.14±10.77	0.67	0.20

Table S4. Cohort features (part 3): lesion characteristics. * = ordinal data presented as mode, other features represented as mean±SD or absolute number (%), presented p-values are the result of univariate analysis using X^2 test for ordinal and categorical features and point-biserial correlation for continuous features, bold **features** have significant p-value ≤ 0.05

Feature	TLF (n=163)	No TLF (n=1811)	Total (1975)	p-value	Missingness [%]
ASA prior to procedure (daily dose) [mg]	71.28±42.67	76.16±52.08	75.75±51.37	0.24	0.15
ASA loading dose [mg]	162±215	125±192	128±194	0.02	0.15
Heparin bolus injection prior to procedure [I.U]	3080±3685	2594±3325	2634±3356	0.08	0.15
Heparin during procedure	4161±3426	5567±2340	5450±3101	0.51	0.20
Anti-platelet medication prior to procedure (daily dose) [mg]	36.55±58.37	49.23±75.39	48.18±74.20	0.04	0.2
Anti-platelet medication loading dose	295±261	252±285	256±285	0.06	0.25

Table S5. Cohort features (part 4): medication. Features represented as mean±SD, presented p-values are the result of univariate analysis using point-biserial correlation, bold **features** have significant p-value ≤0.05

Feature		TLF (n=163)	No TLF (n=1811)	Total (n=1975)	p-value	Missingness [%]
Troponin [μg/L]	7.21±53.59	27.17±294.71	25.6±283.36	0.48	28.41	
Troponin [μg/L] clinical significant?	86 (52.44%)	1014 (55.90%)	1100 (55.61%)	0.96	28.41	
Troponin [μg/L] out of normal range?	6 (3.66%)	118 (6.50%)	124 (6.27%)	0.19	28.41	
Ischemic status	CCS Class of stable angina (n=86)*	2	2	2	0.12	0.25
	Unstable angina	0 (0.00%)	6 (0.33%)	6 (0.30%)	0.46	0.25
	Silent ischemia	0 (0.00%)	2 (0.11%)	2 (0.10%)	0.67	0.25

Table S6. Cohort features (part 5: discharge information. * = ordinal data presented as mode, other features represented as mean±SD or absolute number (%), presented p-values are the result of univariate analysis using X^2 test for ordinal and categorical features and point-biserial correlation for continuous features, bold **features** have significant p-value ≤0.05

Ordinal feature	Code	Category
EQ5D questionnaire	1	No problem
	2	Some problems/moderate feeling
	3	Unable/extreme feeling
	9	Patient did not answer
Pre-procedure TIMI flow [grade]	0	Grade 0 (No perfusion)
	1	Grade 1 (Penetration without perfusion)
	2	Grade 2 (Partial perfusion)
	3	Grade 3 (Complete perfusion)
ACC / AHA lesion characterization	1	Type A
	2	Type B1
	3	Type B2
	4	Type C
CCS Class of stable angina	0	Grade 0 (Myocardial ischemia without any symptoms)
	1	Grade I (Symptoms only with heavy physical activity)
	2	Grade II (Slight restriction of everyday ("ordinary") activity)
	3	Grade III (Significant restriction of daily activity)
	4	Grade IV (Symptoms already at rest)
LVEF class	1	Normal($\geq 55.0\%$)
	2	Mildly reduced (45.0-54.0%)
	3	Moderately reduced (30.0-44.0%)
	4	Severely reduced ($< 30.0\%$)

Table S7. Explanation of ordinal features. LVEF = left ventricular ejection fraction

Classifier	Model structure
ERT	quantile_transformer KNN_imputer smote no_normalizer no_PCA ERT
GB	quantile_transformer KNN_imputer smote no_normalizer no_PCA GB
GP	quantile_transformer KNN_imputer smote l2_normalizer no_PCA GP
KNN	quantile_transformer KNN_imputer smote no_normalizer PCA KNN
L1-LR	quantile_transformer KNN_imputer smote l2_normalizer no_PCA L1-LR
L2-LR	quantile_transformer KNN_imputer smote l2_normalizer no_PCA L2-LR
MLP	quantile_transformer KNN_imputer smote l2_normalizer no_PCA MLP
RF	quantile_transformer KNN_imputer smote no_normalizer no_PCA RF
SVM	quantile_transformer KNN_imputer smote l2_normalizer no_PCA SVM
SL	no_transformer no_imputer smote no_normalizer no_PCA L1-LR

Table S8. Model structure for final TLF models. GB = Gradient Boosting, L1-LR = logistic regression with l1 regularization. L2-LR = logistic regression with L2 regularization, SL = superlearner based on L1-LR.

Algorithm	Fixed hyper-parameters	Range of tuned hyper-parameters
Quantile transformer	<i>output_distribution</i> ="uniform"	None
KNN imputer	None	<i>n_neighbors</i> : [3*, 13*, 23*, 33, 43] <i>weights</i> : ["distance"*, "uniform"*)]
L2 normalizer	None	None
SMOTE	<i>sampling_strategy</i> ="auto"	<i>k_neighbors</i> : [3*, 13*, 23*, 33, 43]
PCA	<i>n_components</i> ="mle" <i>svd_solver</i> ="full"	<i>whiten</i> : ["True", "False"*)]
ERT	<i>criterion</i> ="gini"	<i>n_estimators</i> : [10*, 20, 30, 50, 100] <i>min_sample_leaf</i> : [1, 10, 20, 30, 50, 60*, 70, 100] <i>max_features</i> : ["sqrt", "log2"*)] <i>min_samples_split</i> : [2*, 4]
GB	<i>criterion</i> ="friedman_mse"	<i>learning_rate</i> : [0.001, 0.01*, 0.1*, 0.2, 0.3] <i>n_estimators</i> : [10, 20, 30, 50*, 80*, 100] <i>min_samples_leaf</i> : [1, 10, 20, 30, 50, 60*, 70, 100] <i>max_features</i> : ["sqrt"*, "log2"*)]
GP	None	None
KNN	<i>weights</i> ="uniform"	<i>n_neighbors</i> : [3, 13, 23, 33, 43*, 53*, 63]
L1-LR	<i>penalty</i> ="l1" <i>solver</i> ="saga"	<i>C</i> : [0.01, 0.1, 1*, 10]
L2-LR	<i>penalty</i> ="l2" <i>solver</i> ="lbfgs"	<i>C</i> : [0.001, 0.01*, 0.1*, 1]
MLP	<i>solver</i> ="adam" <i>learning_rate</i> ="adaptive" <i>batch_size</i> =64 <i>early_stopping</i> =True	<i>hidden_layer_size</i> =2 layers from [10, 50, 100] <i>activation</i> : ["tanh"*, "relu"]
RF	<i>criterion</i> ="gini"	<i>n_estimators</i> : [10*, 20, 30, 50, 100] <i>min_sample_leaf</i> : [1, 10, 20, 30, 50, 60*, 70*, 100] <i>max_features</i> : ["sqrt"*, "log2"*)] <i>min_samples_split</i> : [2*, 4]
SVM	<i>probability</i> ="True" <i>decision_function_shape</i> ="ovr" <i>kernel</i> ="rbf"	<i>C</i> : [1, 10*, 50, 100*] <i>gamma</i> : ["auto"*, 0.001, 0.01*]

Table S9. Fixed and tuned hyper-parameters for TLF models. List of techniques, fixed hyper-parameters and the ranges of hyper-parameters tuned during inner cross-validation (splits=4). The hyper-parameters are named according to their implementation in the scikit-learn python library. The hyper-parameters not included in this list are the default settings initialized by the scikit-learn method. The optimization of the hyper-parameters was performed with an exhaustive grid search. GB: Gradient Boosting, L1-LR: logistic regression with l1 regularization. L2-LR: logistic regression with L2 regularization. * denotes the best combination of parameters for the selected models. For MLP best model architecture per split: 1. (10,10), 2. (50,10), 3. (50,10), 4. (100,10), 5. (10,10).

References

1. WHO. The top 10 causes of death.
<https://www.who.int/news-room/fact-sheets/detail/the-top-10-causes-of-death>, 2018.
Accessed: 2021-07-27.
2. Lam, C.S.P.; Voors, A.A.; de Boer, R.A.; Solomon, S.D.; van Veldhuisen, D.J. Heart failure with preserved ejection fraction: from mechanisms to therapies. *Eur. Heart J.* **2018**, *39*, 2780–2792.
3. Baumbach, A.; Bourantas, C.V.; Serruys, P.W.; Wijns, W. The year in cardiology: coronary interventions: The year in cardiology 2019. *European Heart Journal* **2020**, *41*, 394–405.
4. Huber, K.; Ulmer, H.; Lang, I.M.; Mühlberger, Volker, o.b.o.t.A.N.C.R.A. Coronary interventions in Austria, Germany, and Switzerland. *European Heart Journal* **2020**, *41*, 2599–2600.
5. Argulian, E.; Sud, K.; Vogel, B.; Bohra, C.; Garg, V.P.; Talebi, S.; Lerakis, S.; Narula, J. Right Ventricular Dilation in Hospitalized Patients With COVID-19 Infection. *JACC Cardiovasc Imaging* **2020**, *13*, 2459–2461.
6. Kolossváry, M.; Karády, J.; Szilveszter, B.; Kitslaar, P.; Hoffmann, U.; Merkely, B.; Maurovich-Horvat, P. Radiomic Features Are Superior to Conventional Quantitative Computed Tomographic Metrics to Identify Coronary Plaques With Napkin-Ring Sign. *Circ Cardiovasc Imaging* **2017**, *10*.
7. Le, E.P.V.; Rundo, L.; Tarkin, J.M.; Evans, N.R.; Chowdhury, M.M.; Coughlin, P.A.; Pavay, H.; Wall, C.; Zaccagna, F.; Gallagher, F.A.; Huang, Y.; Sriranjani, R.; Le, A.; Weir-McCall, J.R.; Roberts, M.; Gilbert, F.J.; Warburton, E.A.; Schönlieb, C.B.; Sala, E.; Rudd, J.H.F. Assessing robustness of carotid artery CT angiography radiomics in the identification of culprit lesions in cerebrovascular events. *Sci Rep* **2021**, *11*, 3499.
8. Militello, C.; Rundo, L.; Toia, P.; Conti, V.; Russo, G.; Filorizzo, C.; Maffei, E.; Cademartiri, F.; La Grutta, L.; Midiri, M.; Vitabile, S. A semi-automatic approach for epicardial adipose tissue segmentation and quantification on cardiac CT scans. *Comput Biol Med* **2019**, *114*, 103424.
9. Garcia-Garcia, H.M.; McFadden, E.P.; Farb, A.; Mehran, R.; Stone, G.W.; Spertus, J.; Onuma, Y.; Morel, M.A.; van Es, G.A.; Zuckerman, B.; Fearon, W.F.; Taggart, D.; Kappetein, A.P.; Krucoff, M.W.; Vranckx, P.; Windecker, S.; Cutlip, D.; Serruys, P.W. Standardized End Point Definitions for Coronary Intervention Trials: The Academic Research Consortium-2 Consensus Document. *Circulation* **2018**, *137*, 2635–2650.
10. Verheye, S.; Wlodarczak, A.; Montorsi, P.; Torzewski, J.; Bennett, J.; Haude, M.; Starmer, G.; Buck, T.; Wiemer, M.; Nuruddin, A.A.B.; Yan, B.P.; Lee, M.K. BIOSOLVE-IV-registry: Safety and performance of the Magmaris scaffold: 12-month outcomes of the first cohort of 1,075 patients. *Catheter Cardiovasc Interv* **2021**, *98*, E1–E8.
11. Singh, M.; Gersh, B.J.; McClelland, R.L.; Ho, K.K.; Willerson, J.T.; Penny, W.F.; Holmes, D.R. Clinical and Angiographic Predictors of Restenosis After Percutaneous Coronary Intervention. *Circulation* **2004**, *109*, 2727–2731.
12. D’Agostino, R.B.; Vasan, R.S.; Pencina, M.J.; Wolf, P.A.; Cobain, M.; Massaro, J.M.; Kannel, W.B. General Cardiovascular Risk Profile for Use in Primary Care. *Circulation* **2008**, *118*, e86–e86.
13. Piepoli, M.F.; Hoes, A.W.; Agewall, S.; Albus, C.; Brotons, C.; Catapano, A.L.; Cooney, M.T.; Corrà, U.; Cosyns, B.; Deaton, C.; Graham, I.; Hall, M.S.; Hobbs, F.D.R.; Løchen, M.L.; Löllgen, H.; Marques-Vidal, P.; Perk, J.; Prescott, E.; Redon, J.; Richter, D.J.; Sattar, N.; Smulders, Y.; Tiberi, M.; Bart van der Worp, H.; van Dis, I.; Verschuren, W.M.M. 2016 European Guidelines on cardiovascular disease prevention in clinical practice: The Sixth Joint Task Force of the European

Society of Cardiology and Other Societies on Cardiovascular Disease Prevention in Clinical Practice (constituted by representatives of 10 societies and by invited experts) Developed with the special contribution of the European Association for Cardiovascular Prevention & Rehabilitation (EACPR). *Atherosclerosis* **2016**, *252*, 207–274.

14. Anadol, R.; Mühlenhaus, A.; Trieb, A.K.; Polimeni, A.; Münzel, T.; Gori, T. Five Years Outcomes and Predictors of Events in a Single-Center Cohort of Patients Treated with Bioresorbable Coronary Vascular Scaffolds. *Journal of Clinical Medicine* **2020**, *9*.
15. Konigstein, M.; Madhavan, M.V.; Ben-Yehuda, O.; Rahim, H.M.; Srdanovic, I.; Gkargkoulas, F.; Mehdipoor, G.; Shlofmitz, E.; Maehara, A.; Redfors, B.; Gore, A.K.; McAndrew, T.; Stone, G.W.; Ali, Z.A. Incidence and predictors of target lesion failure in patients undergoing contemporary DES implantation: Individual patient data pooled analysis from 6 randomized controlled trials. *American Heart Journal* **2019**, *213*, 105–111.
16. Alaa, A.M.; Bolton, T.; Di Angelantonio, E.; Rudd, J.H.F.; van der Schaar, M. Cardiovascular disease risk prediction using automated machine learning: A prospective study of 423,604 UK Biobank participants. *PLoS ONE* **2019**, *14*, e0213653.
17. Sampedro-Gómez, J.; Dorado-Díaz, P.I.; Vicente-Palacios, V.; Sánchez-Puente, A.; Jiménez-Navarro, M.; Alberto, J.; Galindo-Villardón, P.; Sanchez, P.L.; Fernández-Avilés, F. Machine Learning to Predict Stent Restenosis Based on Daily Demographic, Clinical, and Angiographic Characteristics. *Canadian Journal of Cardiology* **2020**, *36*, 1624–1632.
18. Dorado-Díaz, P.I.; Sampedro-Gómez, J.; Vicente-Palacios, V.; Sanchez, P.L. Applications of Artificial Intelligence in Cardiology. The Future is Already Here. *Rev Esp Cardiol (Engl Ed)* **2019**, *72*, 1065–1075.
19. Rajkomar, A.; Dean, J.; Kohane, I. Machine Learning in Medicine. *N. Engl. J. Med.* **2019**, *380*, 1347–1358.
20. Holmes, D.R.; Savage, M.; LaBlanche, J.M.; Grip, L.; Serruys, P.W.; Fitzgerald, P.; Fischman, D.; Goldberg, S.; Brinker, J.A.; Zeiher, A.M.; Shapiro, L.M.; Willerson, J.; Davis, B.R.; Ferguson, J.J.; Popma, J.; King, S.B.; Lincoff, A.M.; Tchong, J.E.; Chan, R.; Granett, J.R.; Poland, M. Results of Prevention of REStenosis with Tranilast and its Outcomes (PRESTO) trial. *Circulation* **2002**, *106*, 1243–1250.
21. Stolker, J.M.; Kennedy, K.F.; Lindsey, J.B.; Marso, S.P.; Pencina, M.J.; Cutlip, D.E.; Mauri, L.; Kleiman, N.S.; Cohen, D.J. Predicting restenosis of drug-eluting stents placed in real-world clinical practice: derivation and validation of a risk model from the EVENT registry. *Circ Cardiovasc Interv* **2010**, *3*, 327–334.
22. Cassese, S.; Byrne, R.A.; Tada, T.; Pinieck, S.; Joner, M.; Ibrahim, T.; King, L.A.; Fusaro, M.; Laugwitz, K.L.; Kastrati, A. Incidence and predictors of restenosis after coronary stenting in 10004 patients with surveillance angiography. *Heart* **2014**, *100*, 153–159.
23. Ki, Y.J.; Park, K.W.; Kang, J.; Kim, C.H.; Han, J.K.; Yang, H.M.; Kang, H.J.; Koo, B.K.; Kim, H.S. Safety and Efficacy of Second-Generation Drug-Eluting Stents in Real-World Practice: Insights from the Multicenter Grand-DES Registry. *Journal of Interventional Cardiology* **2020**, *2020*, 3872704.
24. Onuma, Y.; Ormiston, J.; Serruys, P.W. Bioresorbable Scaffold Technologies. *Circulation Journal* **2011**, *advpub*, 1102011094–1102011094.
25. Rizik, D.G.; Hermiller, J.B.; Kereiakes, D.J. The ABSORB bioresorbable vascular scaffold: A novel, fully resorbable drug-eluting stent: Current concepts and overview of clinical evidence. *Catheter Cardiovasc Interv* **2015**, *86*, 664–677.

26. Forrestal, B.; Case, B.C.; Yerasi, C.; Musallam, A.; Chezar-Azerrad, C.; Waksman, R. Bioresorbable Scaffolds: Current Technology and Future Perspectives. *Rambam Maimonides Med J* **2020**, *11*.
27. Rapetto, C.; Leoncini, M. Magmaris: a new generation metallic sirolimus-eluting fully bioresorbable scaffold: present status and future perspectives. *Journal of Thoracic Disease* **2017**, *9*.
28. Haude, M.; Ince, H.; Kische, S.; Abizaid, A.; Toelg, R.; Alves Lemos, P.; Van Mieghem, N.M.; Verheye, S.; von Birgelen, C.; Christiansen, E.H.; Barbato, E.; Garcia-Garcia, H.M.; Waksman, R.; BIOSOLVE-II, o.b.o.t.; investigators, I. Safety and clinical performance of a drug eluting absorbable metal scaffold in the treatment of subjects with de novo lesions in native coronary arteries: Pooled 12-month outcomes of BIOSOLVE-II and BIOSOLVE-III. *Catheter Cardiovasc Interventions* **2018**, *92*, E502–E511.
29. Wlodarczak, A.; Garcia, L.A.I.; Karjalainen, P.P.; Komocsi, A.; Pisano, F.; Richter, S.; Lanocha, M.; Rumoroso, J.R.; Leung, K.F. Magnesium 2000 postmarket evaluation: Guideline adherence and intraprocedural performance of a sirolimus-eluting resorbable magnesium scaffold. *Cardiovascular Revascularization Medicine* **2019**, *20*, 1140–1145.
30. Wlodarczak, A.; Starmer, G.; Torzewski, J.; Bennett, J.; Wiemer, M.; Nguyen, M.; Sabate, M.; der Schaaf, R.V.; Montorsi, P.; Eeckhout, E.; Lee, M.K.Y.; Verheye, S. Safety and Performance of the Resorbable Magnesium Scaffold, Magmaris in a Real-World Setting: Analyses of the First Cohort Subjects at 12-Month Follow-up of the BIOSOLVE-IV Registry. *Journal of the American College of Cardiology* **2020**, *76*, B117–B117.
31. Little, R.J.A.; Rubin, D.B. *Statistical Analysis with Missing Data*; John Wiley & Sons, Inc.: USA, 2019.
32. Beretta, L.; Santaniello, A. Nearest neighbor imputation algorithms: a critical evaluation. *BMC Med Inform Decis Mak* **2016**, *16 Suppl 3*, 74.
33. Wulff, J.N.; Jeppesen, L.E. Multiple imputation by chained equations in praxis: guidelines and review. *Electronic Journal of Business Research Methods* **2017**, *15*, 41–56.
34. Stekhoven, D.J.; Bühlmann, P. MissForest—non-parametric missing value imputation for mixed-type data. *Bioinformatics* **2012**, *28*, 112–118.
35. Minka, T. Automatic choice of dimensionality for PCA. *Advances in neural information processing systems* **2000**, *13*, 598–604.